# Hierarchical MPC for coupled subsystems using adjustable tubes $^*$

### Vignesh Raghuraman, Justin P. Koeln

University of Texas at Dallas, Richardson, TX, 75080, United States

### Abstract

A hierarchical Model Predictive Control (MPC) formulation is presented for coupled discrete-time linear systems with state and input constraints. Compared to a centralized approach, a two-level hierarchical controller, with one controller in the upper-level and one controller per subsystem in the lower-level, can significantly reduce the computational cost associated with MPC. Hierarchical coordination is achieved using adjustable tubes, which are optimized by the upper-level controller and bound permissible lower-level controller deviations from the system trajectories determined by the upper-level controller. The size of these adjustable tubes determines the degree of uncertainty between subsystems and directly affects the required constraint tightening under a tube-based robust MPC framework. Sets are represented as zonotopes to enable the ability to optimize the size of these adjustable tubes and perform the necessary constraint tightening online as part of the MPC optimization problems. State and input constraint satisfaction is proven for the two-level hierarchical controller with an arbitrary number of controllers at the lower-level and a numerical example demonstrates the key features and performance of the approach.

Key words: Hierarchical control, Robust model predictive control, Set-based computing, Zonotopes.

### 1 Introduction

Model Predictive Control (MPC) of constrained dynamic systems provides the ability to satisfy both input and state constraints to guarantee safe and reliable system operation. This is particularly important for systems where the desired operation requires both transient and steady-state input and state trajectories to approach these constraints. Examples include the control of water distribution networks [1], aircraft power systems [2], smart power grids [3, 4], and hybrid electric vehicles [5, 6]. However, centralized MPC approaches are not well-suited for the control of these complex multi-timescale systems, where the system is comprised of many dynamically coupled subsystems and achieving the desired operation requires both fast control update rates and long prediction horizons.

For these complex systems, hierarchical MPC can be

Email addresses: vignesh.raghuraman@utdallas.edu (Vignesh Raghuraman), justin.koeln@utdallas.edu (Justin P. Koeln).

used to decompose control decision across multiple levels of controllers [7]. Typically, upper-level controllers are designed with large time step sizes to optimize system operation over long prediction horizons while lower-level controllers use small time step sizes to resolve the fast dynamics of the system over short prediction horizons. With a single controller per level, *vertical* hierarchical MPC is a computationally efficient approach for controlling multi-timescale systems with a relatively low number of states and inputs [8]. For more complex systems, comprised of multiple dynamically-coupled subsystems, *full* hierarchical MPC utilizes multiple controllers at each of the lower-levels to reduce the number of control decisions per controller [9–11].

Many hierarchical MPC formulations [9–12] have been developed to provide theoretical guarantees for the closed-loop system. Specifically, the two-level hierarchical controller in [9] with an upper-level MPC and a lower-level linear controller achieves state and input constraint satisfaction through communication of optimal references and reference rate changes between controller levels and also guarantees closed-loop stability. The controller developed in [12] provides guaranteed persistent controller feasibility and closed-loop stability for a cascaded system with actuator dynamics subject to input constraints. In this case, coordination is achieved

<sup>\*</sup> This material is based upon work supported by the National Science Foundation under Grant No. 1849500. This paper was not presented at any IFAC meeting. Corresponding author J. P. Koeln Tel. +1 972-883-4649. Fax +1 972-883-4659.

through the appropriate choice of contractive terminal constraint sets and terminal control laws, which overall guarantee stability of the error between inner-loop and outer-loop reference models to the origin. The works in [10, 11] extend the vertical hierarchical architecture to a full two-level hierarchical controller with one upper-level controller and multiple controllers at the lower-level, one for each subsystem operating at the same timescale in [10] and different timescales in [11], and guarantees closed-loop stability and input constraint satisfaction while driving the system to a desired steady state. While [10] drives the system to a desired set around a steady-state equilibrium, the works in [9, 11, 12] guarantee convergence to the exact steady-state equilibrium. However, for systems with finite operation, such steadystate equilibrium might not exist, as in the case of systems whose operation is based on the utilization of a finite resource (e.g. battery state of charge in an electric vehicle [6, 13] or fuel in an aircraft [14]).

Similar to [8, 15], this work focuses on the notion of completion, with the goal of maximizing transient performance by satisfying state, input, and terminal constraints during system operation. While the multi-rate hierarchical MPC proposed in [11] achieves real-time computational performance using a full hierarchical MPC architecture with a reduced-order model at the upper-level, guarantees on closed-loop state constraint satisfaction are not shown explicitly. Additionally, the amount of control flexibility provided to the upper- and lower-level controllers along with the resulting uncertainty sets, Robust Positive Invariant (RPI) sets, and tightened constraint sets are determined offline and might not be the optimal choice for systems that need a time-varying control flexibility. Moreover, guaranteed convergence might not be possible for a wide range of systems due to underlying assumptions on the slow timescale of the upper-level controller. To address these challenges, this work focuses on development of a setbased hierarchical MPC architecture for linear systems of dynamically-coupled subsystems that guarantees state and input constraint satisfaction.

One of the fundamental considerations for coordination in hierarchical MPC is how to provide lower-level controllers the flexibility to use their fast update rates and the fast dynamics of the system to improve upon the control decisions made by upper-level controllers without introducing unnecessary conservatism to account for this flexibility. In the authors' prior work [8], set-based vertical hierarchical MPC was proposed, where waysets were used as the primary coordination mechanism to provide both control performance and guaranteed constraint satisfaction. Strategically designed terminal costs were added to complement the waysets to guarantee that the lower-level controllers can only improve control performance compared to the upper-level controller trajectories [16].

For full hierarchical MPC of systems of dynamicallycoupled subsystems, providing lower-level controllers the flexibility to deviate from the trajectories planned by upper-level controllers introduces uncertainty between subsystems. Therefore, the desired degree of flexibility balances the benefits of allowing lower-level controller to improve control performance within their own subsystem with the cost of creating unknown disturbances for neighboring subsystems. This trade off can be timevarying, where certain system operations might require a high level of coordination between subsystems, resulting in very little flexibility for lower-level subsystem controllers to deviate from the upper-level system-wide control plan. Alternatively, other system operations might not require much coordination between subsystems and lower-level controllers should be permitted a high degree of flexibility to further improve control performance.

The proposed two-level hierarchical MPC framework provides this time-varying subsystem coordination flexibility using an adjustable tube set-based coordination mechanism. Specifically, while planning system state and input trajectories, the upper-level controller simultaneously optimizes the permissible deviations from these trajectories provided to the lower-level subsystem controllers and the corresponding constraint tightening needed to be robust to these deviations. These timevarying permissible deviations are communicated to the lower-level controllers that use this flexibility to further optimize subsystem operation. The ability to embed the optimization of these permissible deviation bounds within the upper-level MPC optimization problem is enabled by zonotopes and the recent work on computing RPI sets and Pontryagin difference set operations using linear constraints [17, 18].

The specific contributions of this paper are: (1) the development a two-level hierarchical framework with M lower-level controllers, one for each of the Mdynamically-coupled subsystems; (2) the definition and the use of adjustable tubes to provide time-varying bounds on permissible deviations between upper-level and lower-level planned trajectories; (3) the closed-loop analysis of the hierarchical controller to prove controller feasibility and guarantee constraint satisfaction; and (4) a numerical demonstration of the capabilities of the proposed approach. Note that the proposed work extends the tube-based robust MPC with uncertainty set optimization from [18] to a hierarchical MPC framework with optimal allocation of uncertainty quantified as the differences in control decisions between controller levels and between subsystems. Similar to [18], RPI, tightened output, and tightened terminal sets corresponding to the optimized uncertainty are computed online while solving the control optimization problem.

The remainder of the paper is organized as follows. The notation used throughout the paper is described in Section 2. Sections 3 and 4 describe the class of linear dis-

crete time-invariant systems and the proposed two-level hierarchical MPC formulation. Section 5 presents the nominal system trajectories and error propagation while Section 6 formulates controller feasibility and closed-loop constraint satisfaction. Section 7 demonstrates the key features and performance of the approach using a numerical example. Finally, Section 8 summarizes the conclusions of the paper. Due to space constraints, theorem proofs and additional details for implementing the proposed hierarchical controller are provided in a supplementary technical report [19].

### 2 Notation

For a system comprised of multiple subsystems, systemlevel vectors are denoted in bold, e.g. state  $\mathbf{x}$  and input  $\mathbf{u}$ , while vectors of the  $i^{th}$  subsystem have the subscript i, e.g. state  $x_i$  and input  $u_i$ . The system state vector is formed by the concatenation of subsystem state vectors as  $\mathbf{x} = [x_i]$ . Alternatively, the states of subsystem i can be extracted from the system state vector as  $x_i = \Pi_i \mathbf{x}$ . For a discrete-time system,  $\mathbf{x}(k)$  denotes the state  $\mathbf{x}$  at time step k. With [k, k+N-1] denoting the integers from k to k+N-1, the input trajectory over these time steps is denoted  $\{\mathbf{u}(j)\}_{j=k}^{k+N-1}$ . For MPC, the double index notation  $\mathbf{x}(k+l|k)$  denotes the predicted state at future time k+l determined at time step k. The block-diagonal matrix K with blocks  $K_i$  is denoted  $K = diag(K_i)$ . The p-norm of a vector is denoted  $||\cdot||_p$  and the weighted norm is  $||\mathbf{x}||^2_{\Lambda} = \mathbf{x}^T \Lambda \mathbf{x}$ , where  $\Lambda$  is a positive-definite diagonal matrix. All sets are shown in caligraphic font. For sets  $\mathcal{X}, \mathcal{Y} \in \mathbb{R}^n, \mathcal{X} \oplus \mathcal{Y}$  denotes the Minkowski sum and  $\mathcal{X} \ominus \mathcal{Y}$  denotes the Minkowski/Pontryagin difference of  $\mathcal{Y}$  from  $\mathcal{X}$ . The Cartesian product of sets is denoted as  $\mathcal{X} \times \mathcal{Y}$ . The projection of  $\mathcal{X}$  on the  $n_i$  dimensions of subsystem i is denoted as  $\mathcal{X}_i = \Pi_i \mathcal{X}$ .

### 3 Problem Formulation

Consider a linear discrete time-invariant system composed of M dynamically-coupled subsystems,  $\mathbf{S}_i$ , where  $i \in \mathcal{N} \triangleq [1, M]$ . The dynamics of subsystem  $\mathbf{S}_i$  are

$$x_i(k+1) = A_{ii}x_i(k) + B_{ii}u_i(k) + w_i(k),$$
 (1a)

$$y_i(k) = C_i x_i(k) + D_i u_i(k), \tag{1b}$$

where  $x_i \in \mathbb{R}^{n_i}$  are the states,  $u_i \in \mathbb{R}^{m_i}$  are the inputs, and  $y_i \in \mathbb{R}^{n_i+m_i}$  are the outputs. The coupling between subsystems is captured by the disturbance vector

$$w_i(k) = \sum_{j \in \mathcal{N}_i} (A_{ij} x_j(k) + B_{ij} u_j(k)), \qquad (2)$$

where  $\mathcal{N}_i$  is the set of neighboring subsystems such that

$$\mathcal{N}_i \triangleq \{ j \in \mathcal{N} \setminus \{ i \} : [A_{ij} \ B_{ij}] \neq 0 \}. \tag{3}$$

The outputs are defined to include all states and inputs such that  $y_i(k) \triangleq [x_i(k)^\top u_i(k)^\top]^\top$  and  $[C_i \ D_i] \triangleq I_{n_i+m_i}$ . The subsystem states, inputs, and outputs are constrained such that

$$x_i(k) \in \mathcal{X}_i, \ u_i(k) \in \mathcal{U}_i, \ y_i(k) \in \mathcal{Y}_i \triangleq \mathcal{X}_i \times \mathcal{U}_i.$$
 (4)

Based on (1) and (2), the full system dynamics are

$$\mathbf{x}(k+1) = A\mathbf{x}(k) + B\mathbf{u}(k), \tag{5a}$$

$$\mathbf{y}(k) = C\mathbf{x}(k) + D\mathbf{u}(k), \tag{5b}$$

where  $\mathbf{x} = [x_i] \in \mathbb{R}^n$ ,  $\mathbf{u} = [u_i] \in \mathbb{R}^m$ , and  $\mathbf{y} = [y_i] \in \mathbb{R}^{n+m}$ , such that  $n = \sum_{i=1}^{M} n_i$  and  $m = \sum_{i=1}^{M} m_i$ . The system constraints are

$$\mathbf{x}(k) \in \mathcal{X} \triangleq \mathcal{X}_1 \times \dots \times \mathcal{X}_M,$$
 (6a)

$$\mathbf{u}(k) \in \mathcal{U} \triangleq \mathcal{U}_1 \times \cdots \times \mathcal{U}_M,$$
 (6b)

$$\mathbf{y}(k) \in \mathcal{Y} \triangleq \mathcal{Y}_1 \times \dots \times \mathcal{Y}_M.$$
 (6c)

Let  $A_D \triangleq diag(A_{ii})$  and  $B_D \triangleq diag(B_{ii})$  be block diagonal matrices while  $A_C \triangleq A - A_D$  and  $B_C \triangleq B - B_D$  are off-diagonal matrices that capture the coupling between subsystems.

**Assumption 1** There exists a static feedback control gain  $K_i \in \mathbb{R}^{m_i \times n_i}$  for each subsystem  $\mathbf{S}_i$ ,  $i \in \mathcal{N}$ , such that  $A_{ii} + B_{ii}K_i$  is Schur stable and A + BK is Schur stable, where  $K = diag(K_i)$  is a block-diagonal matrix.

Remark 1 For systems with weak dynamic subsystem coupling, the control gain  $K_i$ ,  $\forall i \in \mathcal{N}$ , satisfying Assumption 1 can often be obtained using decentralized control design methods such as LQR or pole placement. For systems comprised of more strongly coupled subsystems, control gains satisfying Assumption 1 may potentially be found by solving a set of Linear Matrix Inequalities (LMIs) based on [20]. However, for highly-coupled systems, it may not be possible to satisfy Assumption 1 and a control approach that requires the decomposition of the system into subsystems may not be practical.

**Assumption 2** With a fixed time step  $\Delta t$ , the system operates for a finite length of time starting from t=0 and ending at  $t=t_F=k_F\Delta t$  with time steps indexed by  $k \in [0, k_F]$ .

Starting from an initial condition  $\mathbf{x}(0)$ , the goal is to plan and execute an input trajectory and corresponding state and output trajectories satisfying the system dynamics from (5), the constraints from (6) for all  $k \in [0, k_F - 1]$ , and the terminal constraint

$$\mathbf{x}(k_F) \in \mathcal{T} \triangleq \mathcal{T}_1 \times \dots \times \mathcal{T}_M \subseteq \mathcal{X}.$$
 (7)

**Assumption 3** The sets  $\mathcal{X}_i$ ,  $\mathcal{U}_i$ , and  $\mathcal{T}_i$ ,  $i \in \mathcal{N}$ , are zonotopes.

The generic cost function

$$J(\mathbf{x}(0)) = \sum_{j=0}^{k_F - 1} \ell(j) + \ell_F(k_F), \tag{8}$$

defines the cost of system operation using a predetermined reference trajectory  $\{\mathbf{r}(k)\}_{k=0}^{k_F}$  with stage costs  $\ell(j) = \ell(\mathbf{x}(j), \mathbf{u}(j), \mathbf{r}(j))$  and terminal cost  $\ell_F(k_F) = \ell_F(\mathbf{x}(k_F), \mathbf{r}(k_F))$ .

Considering the full system (5), operational constraints (6), terminal constraint (7), and cost function (8), this paper develops a two-level hierarchical control approach with M controllers at the lower-level that guarantees constraint satisfaction and provides computational efficiency in the case of a large number of subsystems M, small time step size  $\Delta t$ , and large operating duration  $t_F$ .

### 4 Hierarchical Control

The proposed hierarchical control formulation consists of a single controller  $C_0$  in the upper-level and M controllers  $C_i$ ,  $i \in \mathcal{N}$ , in the lower-level, where  $C_i$  controls subsystem  $S_i$ .

**Assumption 4** The controller  $C_0$  has a time step size  $\Delta t_0$  and maximum prediction horizon  $\bar{N}_0$  such that  $\Delta t_0 \bar{N}_0 = t_F$ . Each controller  $C_i$ ,  $i \in \mathcal{N}$ , has a time step size  $\Delta t$  and maximum prediction horizon  $\bar{N}$  such that  $\Delta t \bar{N} = \Delta t_0$ .

Let  $\nu_0 \triangleq \frac{\Delta t_0}{\Delta t} = \bar{N} \in \mathbb{Z}_+$  be defined as a time scaling factor for  $\mathbf{C}_0$ . The time steps for  $\mathbf{C}_0$  are indexed by  $k_0$ , with  $k_0 \triangleq \frac{k}{\nu_0}$ , and let  $k_{0,F} \triangleq \frac{k_F}{\nu_0} = \bar{N}_0$  denote the terminal step of  $\mathbf{C}_0$  such that  $k_0 \in [0, k_{0,F}]$ . Thus, the upper-level controller  $\mathbf{C}_0$  has a shrinking horizon, with time-varying horizon length  $N_0(k_0) \triangleq \bar{N}_0 - k_0$ . Each lower-level controller  $\mathbf{C}_i$  has a shrinking and resetting horizon, with horizon length  $N(k) \triangleq \bar{N} - (k \mod \bar{N})$ . This allows  $\mathbf{C}_i$  to predict between updates of  $\mathbf{C}_0$ , at which point  $(k \mod \bar{N} = 0)$  and the prediction horizon resets back to  $N(k) = \bar{N}$ .

Similar to [8, 21],  $\mathbf{C}_0$  predicts coarse state and input trajectories at time indices  $k_0$  with a large time step size  $\Delta t_0$ . Lower-level controllers  $\mathbf{C}_i$  are permitted bounded deviations from the trajectories planned by  $\mathbf{C}_0$  to further improve control performance using a smaller time step size  $\Delta t$ . Unlike [8, 21], this work addresses the coupling between subsystems. If the lower-level controller  $\mathbf{C}_i$  chooses to deviate from the state and input trajectories planned by  $\mathbf{C}_0$ , these deviations create unknown disturbances that could lead to constraint violations in neighboring subsystems. Therefore, instead of using waysets as in [8, 21], a tube-based coordination mechanism is used to bound the permissible deviations between the

trajectories planned by  $\mathbf{C}_0$  and those planned by  $\mathbf{C}_i$ . Moreover, the size of these permissible deviations is optimized online by  $\mathbf{C}_0$  to balance the flexibility given to lower-level controllers with the potentially time-varying need for close coordination among subsystems.

Specifically, for each subsystem, the sets  $\Delta Z_i(\delta_i^z(k_0))$  and  $\Delta \mathcal{V}_i(\delta_i^v(k_0))$  denote scaled zonotopes that bound the permissible state and input deviations between the trajectories planned by  $\mathbf{C}_0$  and those planned by  $\mathbf{C}_i$ . The scaling vectors can be collected to form the output deviation vector  $\delta_i(k_0) = [\delta_i^z(k_0)^\top \ \delta_i^v(k_0)^\top]^\top$  and the permissible output deviation set

$$\Delta \mathcal{Y}_i(\delta_i(k_0)) = \Delta \mathcal{Z}_i(\delta_i^z(k_0)) \times \Delta \mathcal{V}_i(\delta_i^v(k_0)). \tag{9}$$

To reduce notational complexity, the shorthand  $\Delta \mathcal{Y}_i(k_0) = \Delta \mathcal{Y}_i(\delta_i(k_0))$  is used when explicitly stating the dependency on  $\delta_i(k_0)$  is unnecessary. The system state, input, and output deviation vectors are  $\boldsymbol{\delta}^z(k_0) = [\delta_i^z(k_0)], \ \boldsymbol{\delta}^v(k_0) = [\delta_i^v(k_0)], \$ and  $\boldsymbol{\delta}(k_0) = [\boldsymbol{\delta}^z(k_0)^\top \ \boldsymbol{\delta}^v(k_0)^\top]^\top$  and the scaled subsystem deviation sets combine to form the scaled system deviation sets

$$\Delta \mathcal{Z}(\boldsymbol{\delta}(k_0)) = \Delta \mathcal{Z}_1(k_0) \times \cdots \times \Delta \mathcal{Z}_M(k_0), \quad (10a)$$

$$\Delta \mathcal{V}(\boldsymbol{\delta}(k_0)) = \Delta \mathcal{V}_1(k_0) \times \cdots \times \Delta \mathcal{V}_M(k_0), \quad (10b)$$

$$\Delta \mathcal{Y}(\boldsymbol{\delta}(k_0)) = \Delta \mathcal{Z}(\boldsymbol{\delta}(k_0)) \times \Delta \mathcal{V}(\boldsymbol{\delta}(k_0)). \tag{10c}$$

The controller  $C_0$  updates only when  $k = \nu_0 k_0$  (i.e. when  $k \mod \nu_0 = 0$ ), by solving the constrained optimization problem  $P_0(\mathbf{x}(k))$  defined as

$$J_0^* \left( \mathbf{x}(k) \right) = \min_{\substack{\hat{\mathbf{x}}(k_0|k_0), \, \hat{\mathbf{U}}(k_0), \\ \boldsymbol{\delta}(k_0)}} \sum_{j=k_0}^{k_{0,F}-1} \ell\left(j|k_0\right) + \ell_F(k_{0,F}), \quad (11a)$$

 $\text{s.t.} \forall j \in [k_0, k_{0,F} - 1],$ 

$$\hat{\mathbf{x}}(j+1|k_0) = A_0 \hat{\mathbf{x}}(j|k_0) + B_0 \hat{\mathbf{u}}(j|k_0), \tag{11b}$$

$$\hat{\mathbf{y}}(j|k_0) = C\hat{\mathbf{x}}(j|k_0) + D\hat{\mathbf{u}}(j|k_0) \in \hat{\mathcal{Y}}_0(\boldsymbol{\delta}(k_0)), \tag{11c}$$

$$\hat{\mathbf{x}}(k_{0|F}|k_0) \in \hat{\mathcal{T}}_0(\boldsymbol{\delta}(k_0)),\tag{11d}$$

$$\mathbf{x}(k) - \hat{\mathbf{x}}(k_0|k_0) \in \Delta \mathcal{Z}(\boldsymbol{\delta}(k_0)) \oplus \mathcal{E}_0(\boldsymbol{\delta}(k_0)),$$
 (11e)

$$\Delta \mathcal{Z}(\boldsymbol{\delta}(k_0)) \subseteq \operatorname{Pre}(\Delta \mathcal{Z}(\boldsymbol{\delta}(k_0))).$$
 (11f)

The shrinking horizon of  $\mathbf{P}_0(\mathbf{x}(k))$  is reflected in the summation limits in (11a). The stage costs are defined as  $\ell(j|k_0) = \ell(\mathbf{x}(k), \hat{\mathbf{x}}(j|k_0), \hat{\mathbf{u}}(j|k_0), \delta(k_0), \mathbf{r}_0(j))$  to be a function of the measured state, nominal state, nominal input, permissible deviations for lower-level controllers, and the reference trajectory. The reference trajectory  $\mathbf{r}_0(j)$  can be obtained by downsampling the predetermined reference trajectory  $\mathbf{r}(j)$  either using averaging or zero order hold [21]. The terminal cost  $\ell_F(k_{0,F})$  is the same as in (8). Note that the system performance can be balanced with the maximization of  $\boldsymbol{\delta}$  through an additional cost function term  $\Lambda ||\bar{\boldsymbol{\delta}} - \boldsymbol{\delta}||_p$ , where  $\Lambda$  is a

scalar weighting term and  $\bar{\boldsymbol{\delta}}$  is a user-specified upperbound on  $\delta$ . The nominal input trajectory is defined as  $\hat{\mathbf{U}}(k_0) = \{\hat{\mathbf{u}}(j|k_0)\}_{j=k_0}^{k_0,F-1}$ . The permissible deviation scaling vector  $\delta(k_0)$  affects the sizes of the tightened output constraint set  $\hat{\mathcal{Y}}_0(\boldsymbol{\delta}(k_0))$ , the tightened terminal constraint set  $\hat{\mathcal{T}}_0(\boldsymbol{\delta}(k_0))$ , the state deviation constraint set  $\Delta \mathcal{Z}(\boldsymbol{\delta}(k_0))$ , and the RPI set  $\mathcal{E}_0(\boldsymbol{\delta}(k_0))$ , as discussed in Section 5. In (11b), the model used by  $C_0$  assumes a piecewise constant control input over the time step size  $\Delta t_0$  and thus  $A_0 = A^{\nu_0}$  and  $B_0 = \sum_{j=0}^{\nu_0-1} A^j B$  (as in [22]). In (11c) and (11d), the outputs and terminal state are constrained to the time-varying tightened output and terminal constraint sets. Similar to tube-based MPC [23], (11e) allows  $\mathbf{C}_0$  flexibility in the choice of initial condition  $\hat{\mathbf{x}}(k_0|k_0)$ , which is used to prove recursive feasibility of  $\mathbf{P}_0(\mathbf{x}(k))$  (see the proof of Lemma 5 in [19] for details). Finally, (11f) constrains the time-varying permissible state deviation set to be a subset of its own precursor set. Based on the definition from [24], the precursor set is defined specifically as

$$\operatorname{Pre}(\Delta \mathcal{Z}(k_0)) = \left\{ \mathbf{z} \mid \frac{\exists \mathbf{v} \in \Delta \mathcal{V}(k_0) \text{ s.t.}}{A_D \mathbf{z} + B_D \mathbf{v} \in \Delta \mathcal{Z}(k_0)} \right\}, \quad (12)$$

and is used to establish feasibility of the lower-level controllers (see the proof of Lemma 3 in [19] for details). Note that the RPI set  $\mathcal{E}_0(\boldsymbol{\delta}(k_0))$  is assumed to be a *structured* RPI set such that

$$\mathcal{E}_0(\boldsymbol{\delta}(k_0)) = \mathcal{E}_1(\delta_1(k_0)) \times \cdots \times \mathcal{E}_M(\delta_M(k_0)), \quad (13)$$

and is formulated in more detail in Section 5. This structure has been used in distributed robust MPC [25] and imposes an inherent limit on the coupling between subsystems.

The lower-level controllers  $\mathbf{C}_i$ ,  $i \in \mathcal{N}$ , update at each time index k by each solving, in parallel, the constrained optimization problems  $\mathbf{P}_i(x_i(k))$ , defined as

$$J_i^*(x_i(k)) = \min_{\substack{z_i(k|k), \\ V_i(k)}} \sum_{j=k}^{k+N(k)-1} \ell_i(j|k) + \ell_{i,F}(k+N(k)), \quad (14a)$$

s.t. 
$$\forall j \in [k, k + N(k) - 1],$$
  
 $z_i(j+1|k) = A_{ii}z_i(j|k) + B_{ii}v_i(j|k) + \hat{w}_i^*(j),$  (14b)

$$y_i(j|k) = C_i z_i(j|k) + D_i v_i(j|k), \qquad (14c)$$

$$y_i(j|k) - \hat{y}_i^*(j) \in \Delta \mathcal{Y}_i(\delta_i^*(k_0)), \tag{14d}$$

$$z_i(k+N(k)|k) - \hat{x}_i^*(k+N(k)) \in \Delta \mathcal{Z}_i(\delta_i^*(k_0)), \quad (14e)$$

$$x_i(k) - z_i(k|k) \in \mathcal{E}_i(\delta_i^*(k_0)). \tag{14f}$$

The shrinking and resetting horizon of  $\mathbf{P}_i(x_i(k))$  is reflected in the summation limits in (14a). The stage costs are defined as  $\ell_i(j|k) = \ell_i(x_i(k), z_i(j|k), v_i(j|k), r_i(j))$  to be a function of the measured subsystem state, nomi-

nal subsystem state, nominal subsystem input, and subsystem reference trajectory. The terminal cost is defined as  $\ell_{i,F}(k+N(k)) = \ell_{i,F}(z_i(k+N(k)|k), r_i(k+N(k)))$ . The nominal input trajectory is defined as  $V_i(k) = \{v_i(j|k)\}_{j=k}^{k+N(k)-1}$ . In (14b), the subsystem dynamics from (1a) are used with a time-varying  $\mathbf{C}_0$ -optimal disturbance  $\hat{w}_i^*(j)$  that is communicated from  $\mathbf{C}_0$  (details in Section 5). Nominal subsystem outputs are defined in (14c) and the differences between these outputs and the  $\mathbf{C}_0$ -optimal outputs  $\hat{y}_i^*(j)$  are constrained in (14d) to the time-varying permissible output deviation set  $\Delta \mathcal{Y}_i(\delta_i^*(k_0))$  (details in Section 5). Similarly, the difference between the nominal terminal state and the  $\mathbf{C}_0$ -optimal terminal state is constrained to the time-varying permissible state deviation set  $\Delta \mathcal{Z}_i(\delta_i^*(k_0))$  in (14e). Finally, (14f) provides flexibility in initial condition  $z_i(k|k)$  based on the RPI set from (13).

As shown in Fig. 1, coordination between the upper-level controller  $\mathbf{C}_0$  and lower-level controllers  $\mathbf{C}_i$ ,  $i \in \mathcal{N}$ , is achieved through the communication of the  $\mathbf{C}_0$ -optimal trajectories  $\hat{y}_i^*(j)$  and  $\hat{w}_i^*(j)$ ,  $j \in [k, k+N(k)-1]$ , terminal state  $\hat{x}_i^*(k+N(k))$ , and the time-varying permissible deviation vectors  $\delta_i^*(k_0)$ . In this hierarchical control architecture, only the lower-level controllers  $\mathbf{C}_i$  directly affect the system through inputs to the subsystems  $\mathbf{S}_i$ . Once each  $\mathbf{C}_i$  has solved for the optimal nominal input trajectories  $V_i^*(k)$  and optimal nominal initial condition  $z_i^*(k|k)$ , the input to the system is  $\mathbf{u}(k) = [u_i(k)]$  where

$$u_i(k) = v_i^*(k|k) + K_i(x_i(k) - z_i^*(k|k)).$$
 (15)

The two-level hierarchical controller is implemented based on **Algorithm 1**. The specific formulation of the sets in (11) and (14) are presented in Section 5 and the corresponding constraints are used to guarantee satisfaction of the state, input, and terminal constraints from (6) and (7) in Section 6 (see [19] for the associated proofs).

## **Algorithm 1:** Two-level Hierarchical MPC with subsystem coupling.

```
1 Initialize k, k_0 \leftarrow 0

2 if k \mod \nu_0 = 0 then

3 | solve \mathbf{P}_0(\mathbf{x}(k));

4 | communicate \{\hat{y}_i^*(j)\}_{j=k}^{k+N(k)-1},

\{\hat{w}_i^*(j)\}_{j=k}^{k+N(k)-1}, \hat{x}_i^*(k+N(k)), \text{ and } \delta_i^*(k_0)

to \mathbf{P}_i(x_i(k)), \forall i \in \mathcal{N};

5 | k_0 \leftarrow k_0 + 1;

6 end

7 solve \mathbf{P}_i(x_i(k)), \forall i \in \mathcal{N}, and apply the input

\mathbf{u}(k) = [u_i(k)] to the system based on (15);

8 k \leftarrow k + 1:
```

### 5 Nominal Trajectories and Error Propagation

Following the tube-based MPC framework in [23], the goal of this section is to explicitly bound the differences between the nominal trajectories planned by the controllers  $\mathbf{C}_0$  and  $\mathbf{C}_i$ ,  $i \in \mathcal{N}$ , and true system trajectories.

First, since  $\mathbf{C}_0$  has a larger time step size than  $\mathbf{C}_i$  and system dynamics (i.e.  $\Delta t_0 > \Delta t$ ), the input and state trajectories determined by  $\mathbf{C}_0$  must be upsampled. Let  $\hat{\mathbf{u}}^*(k)$  and  $\hat{\mathbf{x}}^*(k)$  be the upsampled input and state trajectories corresponding to the optimal trajectories determined by  $\mathbf{C}_0$ . Since the model (11b) assumed a piecewise constant input, the upsampled trajectories are computed as the forward simulation of (5a) such that

$$\hat{\mathbf{u}}^*(k) = \hat{\mathbf{u}}^*(k_0|k_0), \tag{16a}$$

$$\hat{\mathbf{x}}^*(k) = A^{k-\nu_0 k_0} \hat{\mathbf{x}}^*(k_0|k_0) + \sum_{j=0}^{k-\nu_0 k_0 - 1} A^j B \hat{\mathbf{u}}^*(k_0|k_0), \quad (16b)$$

for  $k \in [\nu_0 k_0, \nu_0(k_0 + 1) - 1]$ . These trajectories create the  $\mathbf{C}_0$ -optimal output and disturbance trajectories  $\hat{y}_i^*(k)$  and  $\hat{w}_i^*(k)$  used in (14d) and (14b), where  $\hat{u}_i^*(k) = \Pi_i \hat{\mathbf{u}}^*(k), \hat{x}_i^*(k) = \Pi_i \hat{\mathbf{x}}^*(k)$ , and

$$\hat{y}_{i}^{*}(k) = [\hat{x}_{i}^{*}(k)^{\top} \ \hat{u}_{i}^{*}(k)^{\top}]^{\top}, \tag{17a}$$

$$\hat{w}_{i}^{*}(k) = \sum_{j \in \mathcal{N}_{i}} (A_{ij}\hat{x}_{j}^{*}(k) + B_{ij}\hat{u}_{j}^{*}(k)).$$
 (17b)

Let  $\Delta \mathbf{x}(k) = [\Delta x_i(k)], \Delta \mathbf{u}(k) = [\Delta u_i(k)], \text{ and } \Delta \mathbf{y}(k) = [\Delta y_i(k)]$  denote the state, input, and output prediction errors for  $\mathbf{C}_0$ , where

$$\Delta x_i(k) \triangleq x_i(k) - \hat{x}_i^*(k), \quad \Delta u_i(k) \triangleq u_i(k) - \hat{u}_i^*(k),$$
  
$$\Delta y_i(k) \triangleq y_i(k) - \hat{y}_i^*(k) = [\Delta x_i(k)^\top \Delta u_i(k)^\top]^\top.$$

These upper-level prediction errors consist of two parts, corresponding to the planned deviations by lower-level controllers  $C_i$  and the resulting lower-level prediction errors due to coupling between subsystems. Specifically,

$$\Delta x_i(k) = \Delta z_i(k) + e_i(k), \tag{19a}$$

$$\Delta u_i(k) = \Delta v_i(k) + K_i e_i(k), \tag{19b}$$

where

$$\Delta z_i(k) \triangleq z_i(k) - \hat{x}_i^*(k), \ \Delta v_i(k) \triangleq v_i(k) - \hat{u}_i^*(k), \ (20)$$

are the planned deviations and  $e_i(k) \triangleq x_i(k) - z_i(k)$ , are lower-level prediction errors due to the coupling between subsystems. Note that  $K_i e_i(k) = u_i(k) - v_i(k)$  based on the control law from (15).

Lemma 1 Let the disturbance error set be defined as

$$\Delta W = A_C \Delta \mathcal{Z} \oplus B_C \Delta \mathcal{V}. \tag{21}$$

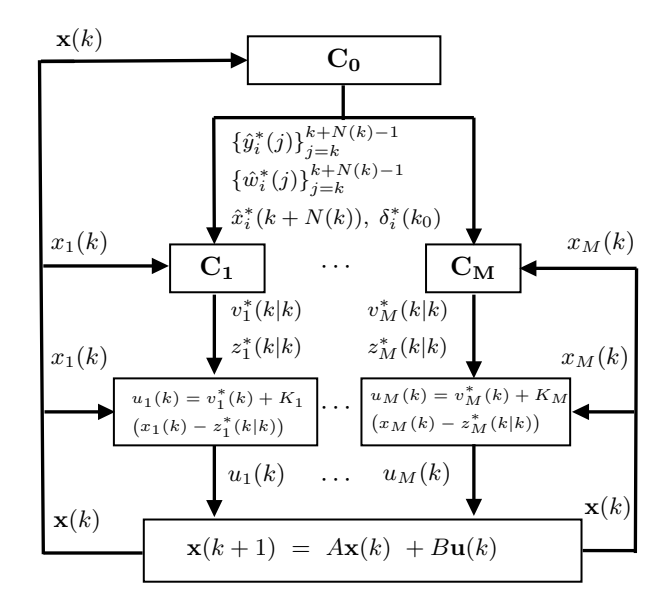


Fig. 1. Two-level hierarchical MPC where  $\mathbf{C}_0$  is formulated based on (11) and  $\mathbf{C}_i$ ,  $i \in \mathcal{N}$ , based on (14). The  $\mathbf{C}_0$ -optimal trajectories  $\hat{y}_i^*(j)$  and  $\hat{w}_i^*(j)$  are computed using (16) and (17). The optimal output deviations  $\delta_i^*(k_0)$  are used to coordinate controllers  $\mathbf{C}_0$  and  $\mathbf{C}_i$ ,  $i \in \mathcal{N}$ , and the static feedback control law (15) computes the inputs to each subsystem  $\mathbf{S}_i$ .

Then the lower-level prediction errors  $\mathbf{e}(k) = [e_i(k)]$  are bounded to the RPI set  $\mathcal{E}_0 \subset \mathbb{R}^n$ , where  $\mathcal{E}_0$  satisfies

$$(A + BK)\mathcal{E}_0 \oplus \Delta \mathcal{W} \subseteq \mathcal{E}_0. \tag{22}$$

The proof of Lemma 1 is constructed based on the evolution of subsystem error dynamics under the static feedback control law from (15) subject to additive unknown but bounded disturbances arising due to permissible subsystem state and input deviations from the upper-level plan as shown in (20) and dynamic subsystem coupling. By concatenating the error dynamics of all subsystems, the disturbances are shown to be bounded to the set  $\Delta W$  from (21), and by constructing  $\mathcal{E}_0$  satisfying (22), proving the claim.

**Lemma 2** The upper-level prediction errors  $\Delta \mathbf{x}(k) = [\Delta x_i(k)]$  and  $\Delta \mathbf{u}(k) = [\Delta u_i(k)]$  are bounded such that

$$\Delta \mathbf{x}(k) \in \Delta \mathcal{Z} \oplus \mathcal{E}_0, \quad \Delta \mathbf{u}(k) \in \Delta \mathcal{V} \oplus K \mathcal{E}_0.$$
 (23)

**PROOF.** The proof follows directly from the definitions of  $\Delta x_i(k)$  and  $\Delta u_i(k)$  from (19) and the result of Lemma 1.

Based on the results of **Lemmas 1** and **2**, the nominal outputs determined by the upper-level controller in (11c) are constrained to the time-varying tightened

output constraint set  $\hat{\mathcal{Y}}_0(\boldsymbol{\delta}(k_0))$ . Then the time-varying tightened output constraint set is defined as

$$\hat{\mathcal{Y}}_0(\boldsymbol{\delta}(k_0)) \triangleq \tilde{\mathcal{Y}}_0 \ominus [(\Delta \mathcal{Z} \oplus \mathcal{E}_0) \times (\Delta \mathcal{V} \oplus K \mathcal{E}_0)], \quad (24)$$

where  $\tilde{\mathcal{Y}}_0 \subseteq \mathcal{Y}$  is a tightened output constraint set used to prevent inter-sample constraint violations (see Appendix A.1 in [19] for details on computing  $\tilde{\mathcal{Y}}_0$ ). Similarly, in (11d), the nominal terminal state is constrained to the time-varying tightened terminal constraint set  $\hat{\mathcal{T}}_0(\boldsymbol{\delta}(k_0))$  defined as

$$\hat{\mathcal{T}}_0(\boldsymbol{\delta}(k_0)) \triangleq \mathcal{T} \ominus (\Delta \mathcal{Z} \oplus \mathcal{E}_0). \tag{25}$$

**Remark 2** While the inter-sample constraint tightening for  $C_0$  could be significant for underdamped higher-order systems, the resulting reduction in control performance can be alleviated through carefully choosing the time step size  $\Delta t_0$  of  $C_0$ , while balancing the overall computational cost associated with a smaller time step size and the maximum prediction horizon  $\bar{N}_0$ .

### 6 Hierarchical Control Feasibility

The following establishes recursive feasibility of each controller in the hierarchy and guarantees constraint satisfaction for the closed-loop system.

**Assumption 5** There exists a feasible solution to  $\mathbf{P}_0(\mathbf{x}(0))$  at time step  $k = k_0 = 0$  for the initial condition  $\mathbf{x}(0)$ .

**Lemma 3** If  $\mathbf{P}_0(\mathbf{x}(k))$  is feasible time step  $k = \nu_0 k_0$ , then  $\mathbf{P}_i(x_i(k)), i \in \mathcal{N}$ , is feasible at this time step.

The proof is structured by first proving the existence of an initial condition  $\mathbf{z}(k|k) = [z_i(k|k)]$  corresponding to the chosen  $\hat{\mathbf{x}}^*(k_0|k_0)$  that simultaneously satisfies (14c) and (14f), and secondly showing the existence of a feasible solution starting from this chosen  $\mathbf{z}(k|k)$ . Using the separable structure of RPI set  $\mathcal{E}_0$  from (13) and  $\Delta \mathcal{Z}$  from (10a), an initial condition  $\mathbf{z}(k|k)$  satisfying the constraints can be determined. With  $z_i(k|k) - \hat{x}_i^*(k) \in \Delta \mathcal{Z}_i(\delta_i^*(k_0))$ ,  $\forall i \in \mathcal{N}$ , a feasible state  $z_i(k+1|k)$  and  $v_i(k|k)$  satisfying (14c) is guaranteed using the definition of precursor set from (12), and by induction, a feasible solution can be constructed through to the terminal time step.

**Lemma 4** For all  $i \in \mathcal{N}$ , if  $\mathbf{P}_i(x_i(k))$  is feasible at time step k, where  $k \mod \nu_0 = 0$  (i.e at the time of  $\mathbf{C}_0$  update), then  $\mathbf{P}_i(x_i(k))$  is feasible at each time step k+1 through k+N(k)-1.

Based on the feasibility of  $\mathbf{P}_i(x_i(k))$ ,  $\forall i \in \mathcal{N}$ , the disturbances are bounded to  $\Delta \mathcal{W}$  and thus,  $x_i(k+1) - z_i^*(k+1|k) \in \mathcal{E}_i(\delta_i^*(k_0))$ ,  $\forall i \in \mathcal{N}$ . Feasible input and

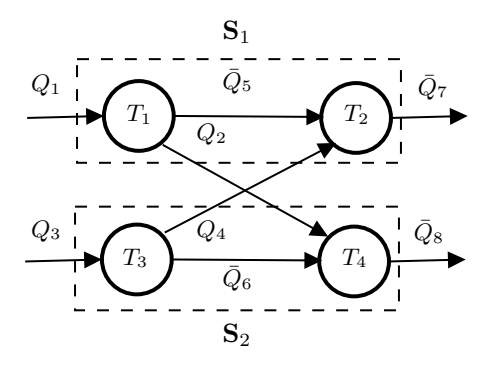


Fig. 2. Thermal system with two subsystems  $S_1$  and  $S_2$  that are dynamically coupled by active power flows  $Q_2$  and  $Q_4$ .

state trajectories correspond to the tails of the optimal sequences determined at previous time step k, and thus,  $\mathbf{P}_i(x_i(k+1)), \forall i \in \mathcal{N}$  is recursively feasible.

**Lemma 5** If  $\mathbf{P}_i(x_i(k-1)) \ \forall i \in \mathcal{N}$  had feasible solutions at the previous time step k-1, then  $\mathbf{P}_0(\mathbf{x}(k))$  has a feasible solution at current time step  $k=\nu_0 k_0$ .

Similar to the proof of **Lemma 4**, the candidate solution is chosen as the optimal nominal state and input sequences corresponding to the tails of the optimal solution determined at previous time step  $k_0 - 1$  and output deviation bound  $\delta^*(k_0 - 1)$ . Note that this candidate solution satisfies (11b), (11c), (11d), and (11f). Additionally,  $\hat{\mathbf{x}}^*(k_0|k_0 - 1)$  is a feasible initial condition based on the feasibility of  $\mathbf{P}_i(x_i(k-1))$ ,  $\forall i \in \mathcal{N}$ , and the invariance of  $\mathcal{E}_i(\delta_i^*(k_0 - 1))$ ,  $\forall i \in \mathcal{N}$ .

**Theorem 1** Following **Algorithm 1** for a two-level hierarchical controller with M controllers in the lower-level, all control problems,  $\mathbf{P}_0(\mathbf{x}(k))$  and  $\mathbf{P}_i(x_i(k))$ ,  $\forall i \in \mathcal{N}$ , are feasible, resulting in system state and input trajectories satisfying state, input, and output constraints from (6) and terminal constraint from (7).

The proof of **Theorem 1** follows from **Assumption 5**, **Lemmas 3-5**, and the output and terminal set constraint tightening from (24) and (25), which are imposed in the upper-level controller through constraints (11c) and (11d).

Remark 3 Note that since the recursive feasibility of the proposed two-level tube-based hierarchical controller is established based only on the constraints (see [19] for the detailed proofs), the objective function can be designed to promote application-specific system operation including reference tracking and economic operation.

### 7 Numerical Example

Consider the four component thermal system shown in Fig. 2 where  $T_i$ ,  $\forall i \in [1, 4]$ , are the temperatures of thermal components, each with thermal capacitance  $C_i$ . The

power flows (heat) into the system  $Q_1$  and  $Q_3$  are controlled directly. Two active power flows  $Q_2$  and  $Q_4$  are controlled by coolant mass flow rates  $\dot{m}_2$  and  $\dot{m}_4$  and satisfy

$$Q_2 = \dot{m}_2 c_p (T_1 - T_4), \quad Q_4 = \dot{m}_4 c_p (T_3 - T_2), \quad (26)$$

where  $c_p$  is the specific heat of the coolant. Additionally, four passive power flows  $\bar{Q}_5$ ,  $\bar{Q}_6$ ,  $\bar{Q}_7$ , and  $\bar{Q}_8$  have constant coolant mass flow rates  $\dot{m}_{p1}$  and  $\dot{m}_{p2}$  and satisfy

$$\bar{Q}_5 = \dot{m}_{p1}c_p(T_1 - T_2), \quad \bar{Q}_6 = \dot{m}_{p1}c_p(T_3 - T_4), \quad (27a)$$
  
 $\bar{Q}_7 = \dot{m}_{p2}c_p(T_2 - T_\infty), \quad \bar{Q}_8 = \dot{m}_{p2}c_p(T_4 - T_\infty). \quad (27b)$ 

From conservation of energy, the nonlinear, continuoustime dynamics are

$$C_1\dot{T}_1 = Q_1 - Q_2 - \bar{Q}_5, \quad C_2\dot{T}_2 = \bar{Q}_5 + Q_4 - \bar{Q}_7, \quad (28a)$$
  
 $C_3\dot{T}_3 = Q_3 - Q_4 - \bar{Q}_6, \quad C_4\dot{T}_4 = \bar{Q}_6 + Q_2 - \bar{Q}_8. \quad (28b)$ 

For the following results,  $C_1=C_2=C_3=C_4=15\times 10^4$  J/K,  $c_p=4181$  J/(kgK), and  $T_\infty=300$  K.

To represent (28a)-(28b) as a linear discrete-time invariant system in the form of (5a), these dynamics are first linearized about nominal mass flow rates  $\dot{m}_2^o = \dot{m}_4^o = 0.036$  kg/s and  $\dot{m}_{p1}^o = \dot{m}_{p2}^o = 0.108$  kg/s, nominal power flow rates  $Q_1^o = Q_3^o = 30$  kW, and nominal temperature differences between adjacent components  $\Delta T^o = 50$  K and then discretized with a time step size of  $\Delta t = 1$  s. As shown in Fig. 2, the system is partitioned into M = 2 subsystems  $\mathbf{S}_1$  and  $\mathbf{S}_2$  with state-input pairs  $[(x_1, x_2), (u_1, u_2)]$  and  $[(x_3, x_4), (u_3, u_4)]$ , respectively. The resulting discrete-time subsystem state and input matrices from (1a) and coupling matrices from (2) are

$$A_{11} = A_{22} = \begin{bmatrix} 0.996 & 0.003 \\ 0.003 & 0.993 \end{bmatrix}, \quad B_{11} = B_{22} = \begin{bmatrix} 7e^{-6} & -1.39 \\ 1e^{-8} & -0.002 \end{bmatrix},$$
 
$$A_{12} = A_{21} = \begin{bmatrix} 0 & 0.001 \\ 0.001 & 0 \end{bmatrix}, \quad B_{12} = B_{21} = \begin{bmatrix} 6e^{-12} & 0.002 \\ 3e^{-9} & 1.39 \end{bmatrix}.$$

The static feedback control gains  $K_1$  and  $K_2$  are designed as discrete-time linear-quadratic regulators with weighting matrices  $Q_i = I_{n_i}$  and  $R_i = 10^5 I_{m_i}$ . The poles of each of the resulting closed-loop subsystems  $\mathbf{S}_1$  and  $\mathbf{S}_2$  are  $\{0.27, 0.99\}$ , while the closed-loop poles of the overall system are  $\{0.12, 0.42, 0.99, 0.99\}$ , and thus, **Assumption 1** is satisfied.

For a two-level hierarchical controller with two subsystems, the system and lower-level controllers  $\mathbf{C}_1$  and  $\mathbf{C}_2$  have time step sizes of  $\Delta t = \Delta t_1 = \Delta t_2 = 1$  s while the upper-level controller  $\mathbf{C}_0$  has time step size of  $\Delta t_0 = 10$ 

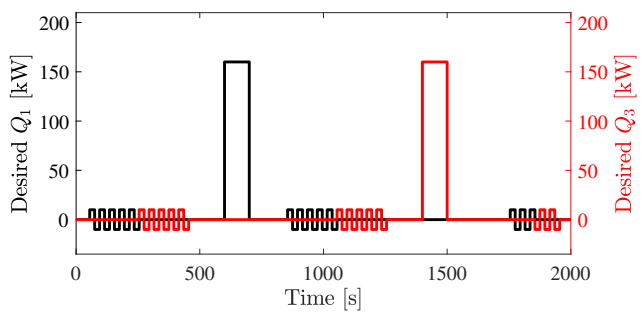


Fig. 3. The desired reference trajectories for  $Q_1$  and  $Q_3$ .

s, which results in  $\nu_0 = 10$ . Thus, the maximum prediction horizons are  $\bar{N}_0 = 200$  and  $\bar{N} = 10$ . The output constraint set  $\mathcal{Y}$  is defined such that  $||\mathbf{x}(k)||_{\infty} \leq 50$  and  $\mathbf{u}(k)$  satisfies

$$\left[ -Q_1^o - \dot{m}_2^o - Q_3^o - \dot{m}_4^o \right]^T \le \mathbf{u}(k) \le \left[ 200 \ 0.14 \ 200 \ 0.14 \right]^T. \tag{30}$$

The terminal constraint set  $\mathcal{T}$  enforces  $||x(k_F)||_{\infty} \leq 50$ . Using the procedure from Appendix A.1 in [19], intersample constraint satisfaction for trajectories planned by  $\mathbf{C}_0$  is achieved using the tightened output constraint set  $\tilde{\mathcal{Y}}_0 = \tilde{\mathcal{X}}_0 \times \mathcal{U}$  where only the state constraints need to be tightened. Minimal tightening is required where  $\tilde{\mathcal{X}}_0 = \{\mathbf{x} \in \mathbb{R}^n \mid \underline{x} \leq \mathbf{x} \leq \overline{x}\}$  is computed such that

$$\underline{x} = \begin{bmatrix} -49.93 & -49.86 & -49.93 & -49.86 \end{bmatrix}^{\top}$$

$$\overline{x} = \begin{bmatrix} 49.88 & 49.91 & 49.88 & 49.91 \end{bmatrix}^{\top}.$$

Given an initial state of  $\mathbf{x}(0) = \mathbf{0}$ , the desired operation defined by  $\{r(k)\}_{k=0}^{k_F}$ , is shown in Fig. 3 for the first input (power flow  $u_1$ ) and third input (power flow  $u_3$ ). References for the second and fourth inputs (mass flow rates  $u_2$  and  $u_4$ ) are the corresponding lower bounds from (30) for the entire operation. The primary objective is to track the desired power flows  $(u_1, u_3)$  into the system while minimizing mass flow rates  $(u_2, u_4)$  and satisfying state and input constraints from (6a) and (6b). For this example, the references for  $\mathbf{C}_0$  are obtained by downsampling the references using averaging. Note that the small high-frequency pulse references for power flows  $u_1$  and  $u_3$  vary in-between the updates of  $\mathbf{C}_0$ .

The weighted quadratic cost function in (8) is defined based on these references and rate of input change as

$$\ell(\mathbf{x}(j), \mathbf{u}(j), \mathbf{r}(j)) = ||\mathbf{r}(j) - \mathbf{u}(j)||_{\Gamma_1}^2 + ||\mathbf{u}(j) - \mathbf{u}(j-1)||_{\Gamma_2}^2,$$
(32)

where  $\Gamma_1={\rm diag}([10^5\ 10^{-2}\ 10^5\ 10^{-2}])$  and  $\Gamma_2={\rm diag}([0\ 10^{-2}\ 0\ 10^{-2}]).$ 

Fig. 4 shows closed-loop simulation results using the linearized system model and the proposed two-level hierar-

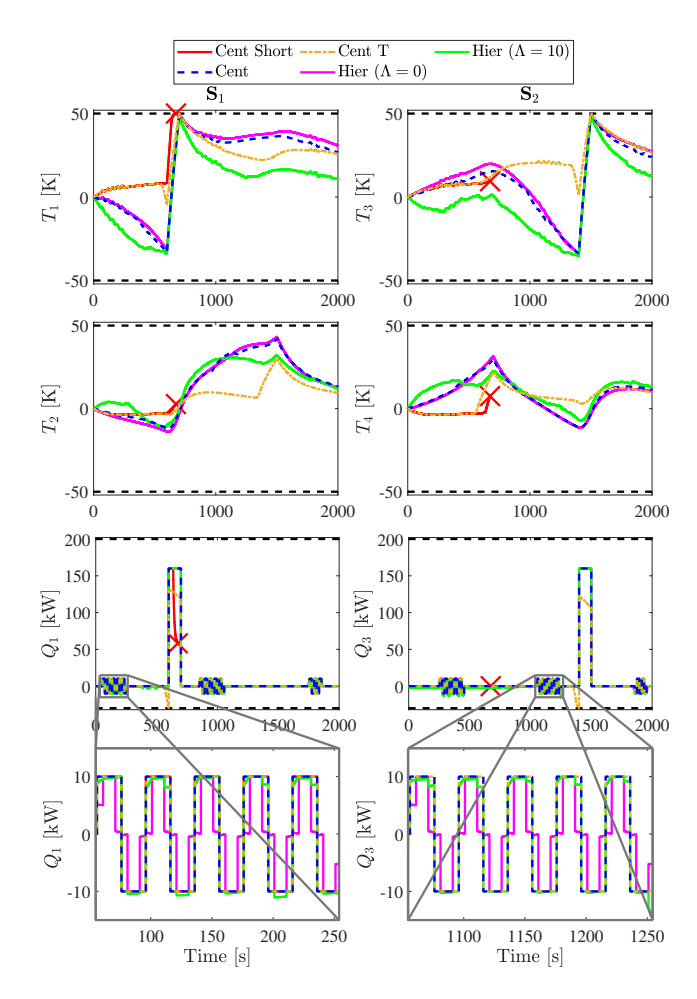


Fig. 4. Simulation results comparing the shrinking horizon centralized controller, receding horizon centralized controller with a short prediction horizon, receding horizon centralized controller with a terminal constraint, two-level hierarchical controller with no subsystem deviations, and a two-level hierarchical controller with subsystem deviations.

chical controller (Hier ( $\Lambda = 10$ )), where  $\Lambda$  is a cost function weighting term used to incentivize maximizing the permissible deviation scaling vector  $\delta(k_0)$ , compared to a two-level hierarchical controller with no subsystem deviations (Hier  $(\Lambda = 0)$ ), a shrinking horizon centralized controller (Cent) that predicts to the end of system operation, a receding horizon centralized controller with a control invariant terminal set and a prediction horizon of N = 100 time steps (Cent T), and a receding horizon centralized controller (Cent Short) with a short prediction horizon of N = 10 time steps. As expected, all the controllers except the Cent Short controller satisfy the state constraints. Since there does not exist a steadystate operating condition that satisfies the state and input constraints while tracking the desired large pulsed power flows  $Q_1$  and  $Q_3$  shown in the third row of subplots in Fig. 4, the controllers strategically precool the system temperatures to utilize the thermal capacitance of the system. Note that due to a short prediction horizon, the Cent T controller is unable to achieve the nec-

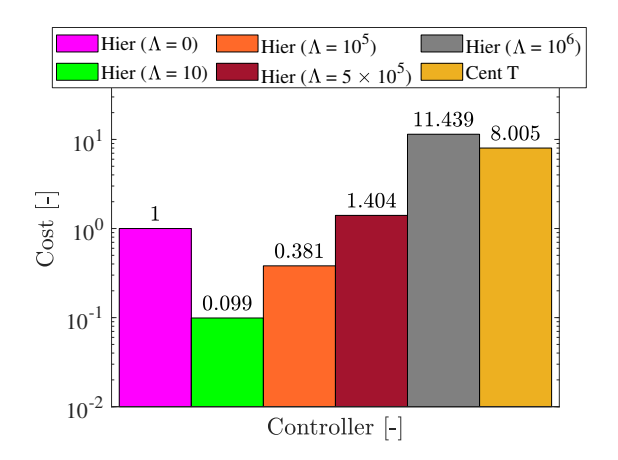


Fig. 5. Relation between the chosen value of  $\Lambda$  and normalized cost relative to Hier ( $\Lambda = 0$ ) computed using (32).

Table 1 Controller computation times

Controller	Computation time (s)		
	Minimum	Mean	Maximum
Cent	13.569	23.144	1092.3
Cent Short	0.009	0.01	0.05
Cent T	0.08	0.09	0.137
Hier $(\mathbf{C}_0)$	0.757	2.262	4.105
Hier $(\mathbf{C}_1,  \mathbf{C}_2)$	0.011	0.014	0.08

essary level of precooling and thus, significantly reduces the power flow into the system to avoid temperature constraint violations. While the Cent controller tracks all pulses of the reference power flows, Hier ( $\Lambda=0$ ) tracks only the large pulse references. The smaller, high-frequency, pulse references are not tracked perfectly by Hier ( $\Lambda=0$ ) due to step changes occurring between updates of  $\mathbf{C}_0$ . Alternatively, Hier ( $\Lambda=10$ ) achieves perfect tracking of the large pulsed power flows and nearly perfect tracking of the small, high-frequency, pulse references by allowing the lower-level controllers to deviate from the upper-level prediction, as shown in bottom row of subplots in Fig. 4 during the time intervals [55, 254] s and [1055, 1254] s, respectively.

Fig. 5 shows the total operating costs computed using (32) when using the proposed hierarchical controller for  $\Lambda = \{10, 10^5, 5 \times 10^5, 10^6\}$  normalized by the cost when using Hier ( $\Lambda = 0$ ). Initially, the normalized costs decreases due to the additional flexibility provided to  $\mathbf{C}_1$  and  $\mathbf{C}_2$  by the increasing size of output deviation sets. However, as shown by Hier ( $\Lambda = 5 \times 10^5$ ), there is a point where further increasing the size of the output deviation sets leads to significant constraint tightening that degrades overall control performance.

Using Yalmip [26] and Gurobi optimizer 8.5 [27] to for-

mulate and solve the controller optimization problems, Table 1 shows the mean, minimum, and maximum computation times for each controller. Note that despite the additional complexity of simultaneous uncertainty set optimization and constraint tightening at  $\mathbf{C}_0$ , the computation time is smaller than that of the Cent controller. Furthermore, the average computation time of  $\mathbf{C}_1$  and  $\mathbf{C}_2$  is similar to Cent Short and less than Cent T. Overall, the proposed hierarchical approach is expected to remain computationally efficient for systems with significantly more states, inputs, and subsystems.

#### 8 Conclusions

A two-level hierarchical MPC formulation was presented for linear systems of dynamically-coupled subsystems. Adjustable tubes are used to bound permissible deviations between the system trajectories planned by the upper- and lower-level controllers. A tube-based robust MPC formulation with simultaneous uncertainty set optimization and constraint tightening guaranteed constraint satisfaction to bounded disturbances between subsystem controllers. A numerical example demonstrated the performance of the proposed two-level hierarchical MPC. Future work will focus on the extension of the proposed set-based hierarchical MPC formulation to nonlinear systems and include more than two levels of controllers with application to systems of greater complexity.

### References

- Ye Wang, Vicenç Puig, and Gabriela Cembrano. Nonlinear economic model predictive control of water distribution networks. *Journal of Process Control*, 56:23–34, 2017.
- [2] Jinwoo Seok, Ilya Kolmanovsky, and Anouck Girard. Coordinated model predictive control of aircraft gas turbine engine and power system. *Journal of Guidance, Control, and Dynamics*, 40(10):2538–2555, 2017.
- [3] Irfan Khan, Zhicheng Li, Yinliang Xu, and Wei Gu. Distributed control algorithm for optimal reactive power control in power grids. *International Journal of Electrical* Power and Energy Systems, 83:505–513, 2016.
- [4] Muhammad Irfan, Jamshed Iqbal, Adeel Iqbal, Zahid Iqbal, Raja Ali Riaz, and Adeel Mehmood. Opportunities and challenges in control of smart grids – Pakistani perspective. Renewable and Sustainable Energy Reviews, 71 (2017):652– 674, 2017.
- [5] Wisdom Enang and Chris Bannister. Modelling and control of hybrid electric vehicles (A comprehensive review). Renewable and Sustainable Energy Reviews, 74:1210–1239, 2017
- [6] Wenqing Wang and Justin P Koeln. Hierarchical Multi-Timescale Energy Management for Hybrid-Electric Aircraft. ASME Dynamic Systems and Control Conference, 2020.
- [7] Riccardo Scattolini. Architectures for distributed and hierarchical Model Predictive Control - A review. *Journal of Process Control*, 19:723–731, 2009.

- [8] Justin P. Koeln, Vignesh Raghuraman, and Brandon M. Hencey. Vertical hierarchical MPC for constrained linear systems. Automatica, 113:108817, 2020.
- [9] Davide Barcelli, Alberto Bemporad, and Giulio Ripaccioli. Hierarchical multi-rate control design for constrained linear systems. Proceedings of the IEEE Conference on Decision and Control, pages 5216–5221, 2010.
- [10] M. Farina, X. Zhang, and R. Scattolini. A hierarchical MPC scheme for interconnected systems. *IFAC-PapersOnLine*, 50(1):12021–12026, 2017.
- [11] Marcello Farina, X. Zhang, and Riccardo Scattolini. A hierarchical multi-rate MPC scheme for inter-connected systems. Automatica, 90:38–46, 2018.
- [12] Chris Vermillion, Amor Menezes, and Ilya Kolmanovsky. Stable hierarchical model predictive control using an inner loop reference model and λ-contractive terminal constraint sets. Automatica, 50(1), 2014.
- [13] Balaji Sampathnarayanan, Simona Onori, and Stephen Yurkovich. An optimal regulation strategy with disturbance rejection for energy management of hybrid electric vehicles. Automatica, 50:128–140, 2014.
- [14] David B Doman. Rapid mission planning for aircraft thermal management. AIAA Guidance, Navigation, and Control Conference, page 1076, 2015.
- [15] Arthur Richards and Jonathan P. How. Model Predictive Control of Vehicle Maneuvers with Guaranteed Completion Time and Robust Feasibility. American Control Conference, pages 4034–4040, 2003.
- [16] Vignesh Raghuraman, Venkatraman Renganathan, Tyler H. Summers, and Justin P. Koeln. Hierarchical MPC with Coordinating Terminal Costs. American Control Conference, pages 4126–4133, 2020.
- [17] Vignesh Raghuraman and Justin P. Koeln. Set operations and order reductions for constrained zonotopes. arXiv:2009.06039v1, 2020.
- [18] Vignesh Raghuraman and Justin P. Koeln. Tubebased robust MPC with adjustable uncertainty sets using zonotopes. American Control Conference, pages 462–469, 2021.
- [19] Vignesh Raghuraman and Justin P. Koeln. Hierarchical MPC for coupled subsystems using adjustable tubes. arXiv:2202.11228, 2022.
- [20] Giulio Betti, Marcello Farina, and Riccardo Scattolini. Realization issues, tuning, and testing of a distributed predictive control algorithm. *Journal of Process Control*, 24(4), 2014.
- [21] Justin P. Koeln and Brandon M. Hencey. Constrained Hierarchical MPC via Zonotopic Waysets. American Control Conference, pages 4237–4244, 2019.
- [22] Riccardo Scattolini and Patrizio Colaneri. Hierarchical model predictive control. Proceedings of the IEEE Conference on Decision and Control, pages 4803–4808, 2007.
- [23] D.Q. Mayne, M.M. Seron, and S.V. Raković. Robust Model Predictive Control of Constrained Linear Systems with Bounded Disturbances. Automatica, 41:219–224, 2005.
- [24] F. Borrelli, A. Bemporad, and M. Morari. Predictive Control for Linear and Hybrid Systems. Cambridge University Press, 2011
- [25] Paul A. Trodden and J. M. Maestre. Distributed predictive control with minimization of mutual disturbances. Automatica, 77:31–43, 2017.

- [26] J. Lofberg. Yalmip: a toolbox for modeling and optimization in matlab. *IEEE International Conference on Robotics and Automation*, pages 284–289, 2005.
- [27] Optimization Gurobi. Gurobi Optimizer Reference Manual.  $\it Gurobi~Optimization~Inc.,~2018.$